# Neoclassical momentum transport in an impure rotating tokamak plasma

S. Newton, and P. Helander

## Articles you may be interested in

Ion transport in toroidally rotating tokamak plasmas
The Physics of Fluids **30**, 2784 (1987); 10.1063/1.866045

Neoclassical transport in a rotating impure plasma
Physics of Plasmas **5**, 1209 (1998); 10.1063/1.872629

Nonlinear neoclassical transport in a rotating impure plasma with large gradients
Physics of Plasmas **6**, 3066 (1999); 10.1063/1.873593

Bootstrap current and neoclassical transport in tokamaks of arbitrary collisionality and aspect ratio
Physics of Plasmas **4**, 3230 (1997); 10.1063/1.872465

Neoclassical poloidal and toroidal rotation in tokamaks
Physics of Fluids B: Plasma Physics **3**, 2050 (1991); 10.1063/1.859671

Neoclassical current in a toroidally-confined multispecies plasma
The Physics of Fluids **21**, 1295 (1978); 10.1063/1.862397

# Neoclassical momentum transport in an impure rotating tokamak plasma

S. Newton
*H. H. Wills Physics Laboratory, University of Bristol, Royal Fort, Tyndall Avenue, Bristol BS8 1TL, United Kingdom*

P. Helander
*EURATOM/UKAEA Fusion Association, Culham Science Centre, Abingdon, Oxfordshire OX14 3DB, United Kingdom*

It is widely believed that transport barriers in tokamak plasmas are caused by radial electric-field shear, which is governed by angular momentum transport. Turbulence is suppressed in the barrier, and ion thermal transport is comparable to the neoclassical prediction, but experimentally angular momentum transport has remained anomalous. With this motivation, the collisional transport matrix is calculated for a low collisionality plasma with collisional impurity ions. The bulk plasma toroidal rotation velocity is taken to be subsonic, but heavy impurities undergo poloidal redistribution due to the centrifugal force. The impurities give rise to off-diagonal terms in the transport matrix, which cause the plasma to rotate spontaneously. At conventional aspect ratio, poloidal impurity redistribution increases the angular momentum flux by a factor up to $\varepsilon^{-3/2}$ over previous predictions, making it comparable to the "banana" regime heat flux. The flux is primarily driven by radial pressure and temperature gradients.
[DOI: 10.1063/1.2160518]

## I. INTRODUCTION

It is widely believed that internal transport barriers (ITBs) form in regions where the radial electric field is strongly sheared. As the radial electric-field profile is controlled by angular momentum transport, if turbulence is suppressed in an ITB, neoclassical angular momentum transport is likely to play a key role in the formation and sustainment of the ITB. Ion thermal transport is observed in ITB plasmas at the neoclassical level,[1,2] predicted by assuming that the bulk ions are in a low collisionality regime, suggesting that turbulence is indeed suppressed. However, experimentally the radial angular momentum transport in these regions has remained anomalous, being typically an order of magnitude larger than the neoclassical prediction[2] and comparable to the ion thermal transport.

Angular momentum is carried predominantly by the bulk ions, so angular momentum transport is determined by the bulk ion viscosity. The neoclassical toroidal viscosity was first calculated for the case of slow toroidal rotation of a pure plasma by Rosenbluth *et al.*[3] Later, Hinton and Wong[4] and Catto *et al.*[5] provided the extension to toroidal rotation at a speed comparable to the ion thermal speed. Despite taking the ion collisionality to be low, the viscosity scaling with aspect ratio was characteristic of the bulk ions being in the collisional, Pfirsch-Schlüter regime and thus was substantially smaller than the heat diffusivity.

Heavy impurities, such as carbon, are usually present in a plasma. Impurities in the region of an ITB may be expected to be in a high charge state and are therefore typically collisional. Hirshman[6] calculated the particle and heat transport in a mixed collisionality plasma, in which the bulk ions were in the low collisionality "banana" regime, and the single impurity species was collisional. He found that the scaling with

aspect ratio of the heat flux was as expected for transport dominated by trapped banana particles, but the particle flux scaling was characteristic of transport by collisional particles, thus making it much smaller than the heat flux.

In a rotating plasma, particles are subject to a centrifugal force, when viewed in a comoving frame, which pushes particles to the outside of the torus. As cross-field transport acts slowly, the particles will accumulate on the outboard side of each flux surface. Due to their large mass, impurities feel a substantial centrifugal force; thus their distribution around a flux surface is expected to be significantly nonuniform (for example, see Wesson[7]), which is seen experimentally.[8] Fülöp and Helander[8] took this redistribution into account in the mixed collisionality plasma considered by Hirshman and found that both the particle and heat fluxes then displayed the scaling with aspect ratio characteristic of the banana regime.

Wong[9] determined the toroidal viscosity for an arbitrarily rotating plasma, with impurity redistribution, in which both the bulk ions and a single impurity species were in the low collisionality banana regime. He found no significant enhancement over the viscosity in a pure plasma. However, the toroidal viscosity has not previously been determined for a mixed collisionality, rotating plasma, with impurity redistribution, which Wong also pointed out at the end of Ref. 9. In this paper we consider the transport in this experimentally relevant condition and find a much more substantial effect than that seen by Wong.

Radial transport may be characterized by the transport matrix $L$ which relates radial gradients of the three plasma parameters, bulk ion pressure $p_i$, bulk ion temperature $T_i$ and toroidal angular velocity $\omega$, to the radial bulk ion flux of particles $\Gamma$, heat $q$, and toroidal angular momentum $\Pi$. We

have calculated the elements of the matrix $L$, including both the classical and neoclassical contributions. The classical transport was determined for a general toroidal rotation velocity, however, we consider here the neoclassical transport only under the condition of subsonic bulk plasma rotation, that is the bulk ion Mach number $M_i^2 = m_i \omega^2 R^2 / 2 T_i \ll 1$, but still allowing the toroidal rotation velocity to exceed the diamagnetic speed. Here $m_i$ is the bulk ion mass, $T_i$ is their temperature, $R$ is the major radius, and $\omega$ is the rotation frequency.

The plasma is assumed to consist of electrons, collisionless hydrogenic ions, and a single, heavy impurity species with a high charge $z \gg 1$, which is therefore collisonal. Taking $\alpha = z^2 n_z / n_i$, where $n_i$ and $n_z$ are the bulk ion and impurity densities, respectively, this requires that $1 \gg \nu_{*i} \gg 1 / \alpha z^2$, where the collisionality $\nu_{*i}$ is the ratio of the bulk ion self-collision frequency to their transit frequency. Experimentally, the frequency of bulk ion self-collisions is typically comparable to that of bulk ion-impurity collisions. This requires that the impurity concentration satisfies $n_z z \ll n_i \sim z^2 n_z$. Due to their large mass $m_z \sim z m_i$, the impurity Mach number $M_z^2 = m_z \omega^2 R^2 / 2 T_z$ will be of order unity, even if $M_i \ll 1$, so significant impurity redistribution is expected.

Following the work of Hinton and Wong, flux-friction relations are used to determine the cross-field transport. Evaluation of the classical transport largely follows the standard procedure introduced by Braginskii. The classical transport is found to be enhanced over that in a pure plasma, due to both the inclusion and redistribution of impurities.

In Refs. 4 and 5 a variational method was employed to evaluate the neoclassical fluxes, however, an alternative approach is presented here. By using an explicit linearized collision operator, whose form is motivated in Sec. III, the ion distribution function is determined to the required order in the appropriate expansion parameters, then used directly to evaluate the expressions for the fluxes. The pressure and temperature gradient driven parts of the neoclassical particle and heat fluxes are seen to agree with those determined previously by other authors. The additional contributions to the fluxes calculated here, driven by rotation shear, are of comparable size to the other terms and we find a thermal pinch driven by rotation shear. The neoclassical angular momentum transport differs significantly from previous expectations. The off-diagonal transport coefficients $L_{31}$ and $L_{32}$ show a scaling with aspect ratio typical of that expected for bulk ions in the banana regime and are the primary driving forces of the angular momentum flux. However, the toroidal viscosity usually inferred from transport codes, essentially the coefficient $L_{33}$, shows only a modest enhancement over previous results and is smaller than $L_{31}$ and $L_{32}$ by a factor of around $M_i^2$.

The paper is organized as follows. In Sec. II, the equations which we use to determine the ion distribution function are obtained by expansion of the Fokker-Planck equation, following Ref. 4, and the expected form of the impurity redistribution is discussed. In Sec. III the adopted collision operator is motivated. Expressions for the radial fluxes are given in Sec. IV, and the classical fluxes are evaluated generally in Sec. V. Then, in Sec. VI, the solution of the drift

kinetic equation for a subsonic plasma is obtained, and the neoclassical fluxes are evaluated. The transport matrix for a subsonic plasma is given in Sec. VII and the behavior of the transport coefficients is analyzed. Finally a discussion is presented in Sec. VIII.

## II. EXPANSION OF THE FOKKER-PLANCK EQUATION

Hinton and Wong, in Ref. 4, established a systematic way of expanding the ion kinetic equation in order to analyze neoclassical transport in a rotating plasma with arbitrary toroidal velocity. In this section, we summarize the results of that work which we will require. The general axisymmetric form for the magnetic field has been assumed: $\mathbf{B} = I \nabla \phi + \nabla \phi \times \nabla \Psi$, where $\Psi$ is the poloidal flux function and $\phi$ is the toroidal angle.

The bulk ion distribution function $f_i$ satisfies the Fokker-Planck equation,

$$\frac{\partial f_i}{\partial t} + \mathbf{v} \cdot \nabla f_i + \frac{e}{m_i}(\mathbf{E} + \mathbf{v} \times \mathbf{B}) \cdot \frac{\partial f_i}{\partial \mathbf{v}} = C_i + S. \quad (1)$$

The symbols have their usual meaning and throughout a subscript $i$ implies a property of the (singly charged) bulk ions. Hinton and Wong transform this equation to a frame moving with the local rotation velocity $\mathbf{u}_0$ which is found to be purely toroidal throughout the time scales we consider

$$\mathbf{u}_0 = \omega(\Psi, t) R \hat{e}_\phi. \quad (2)$$

Here $\hat{e}_\phi$ is a unit vector in the toroidal direction and the angular rotation frequency $\omega$ is constant on a flux surface.

The basic expansion parameter $\delta$ is taken to be the ratio of the ion gyroradius $\rho_i$ to the typical macroscopic radial scale length $L$. A subscript indicates the order of expansion, for example, $f = f_0 + f_1 + \cdots$. $S$ is assumed to be second order at most. To allow the bulk flow velocity to be comparable to the ion thermal speed, the electric field is assumed large—the leading term in its expansion, $\mathbf{E} = \mathbf{E}_{-1} + \mathbf{E}_0 + \mathbf{E}_1 + \cdots$, is of order $T_i / eL\delta$, where $T_i$ is the ion temperature. Thus the electromagnetic terms in the Fokker-Planck equation approximately balance. With the assumption that the magnetic field is not changing on the time scales of interest, the electric field is given by an electrostatic potential: $\mathbf{E}_{-1} = -\nabla \Phi_{-1}$ and $\mathbf{E}_0 = -\nabla \Phi_0$. Hinton and Wong showed that $\Phi_{-1}$ is constant around a flux surface, whilst $\Phi_0$ has a poloidal dependence, and that the rotation frequency is related to the potential via $\omega = -\partial \Phi_{-1} / \partial \Psi$. We will include the flux-surface average of $\Phi_0$ in $\Phi_{-1}$, so $\Phi_0$ is replaced by $\tilde{\Phi}_0$, the leading order poloidal variation of the electrostatic potential, which has a flux-surface average of zero.

Hinton and Wong showed that the lowest-order distribution function for each species quickly relaxes to a Maxwellian,

$$f_0 = n_0 \left( \frac{1}{\pi v_T^2} \right)^{3/2} e^{-(v'^2/v_T^2)}, \quad (3)$$

where $\mathbf{v}' = \mathbf{v} - \omega R \hat{e}_\phi$ is the velocity in the rotating frame, $v_T^2 = 2T/m$ is the thermal velocity of the species, where the species' temperature is a flux-surface function, and $n_0 = \int d^3v f_0$ is

the zeroth-order density. The velocity moment of $f_0$ in the laboratory frame is $\mathbf{u}_0$ for all species.

The first-order correction to the distribution function consists of two parts: a classical, gyrophase-dependent piece $\tilde{f}_1$, and a neoclassical piece $\bar{f}_1$ obtained from a drift kinetic equation. Noting that the parallel and perpendicular subscripts refer to the direction of the magnetic field, it is useful to use cylindrical velocity coordinates $v_\parallel$, $v_\perp$ and the gyroangle $\zeta$ in the rotating frame, such that

$$\mathbf{v}' = \hat{b}v_\parallel + \mathbf{v}_\perp \tag{4}$$

and

$$\mathbf{v}_\perp = v_\perp(\hat{e}_1 \cos \zeta + \hat{e}_2 \sin \zeta), \tag{5}$$

where $\hat{b} = \mathbf{B}/B \equiv \hat{e}_3$ and $\hat{e}_1$, $\hat{e}_2$ are two other, mutually orthogonal, unit vectors, with $\hat{e}_1$ parallel to $\nabla\Psi$. The magnetic moment and energy of a particle with charge $q$ in the rotating frame are

$$\mu = mv_\perp^2/2B \tag{6}$$

and

$$H = \frac{m}{2}(v_\parallel^2 + v_\perp^2) + q\tilde{\Phi}_0 - \frac{m\omega^2 R^2}{2}. \tag{7}$$

The gyrophase-dependent part of the distribution function is independent of collisionality. An explicit expression was obtained by Hinton and Wong, which is valid for any species, recognizing that the subscript then refers to an expansion in the ratio of that species' gyroradius to $L$. Using a prime on a scalar quantity to indicate the derivative with respect to $\Psi$,

$$\tilde{f}_1 = \frac{v_\perp \sin \zeta |\nabla\Psi|}{\Omega}\left[\frac{N'}{N} + \left(\frac{H}{T} - \frac{3}{2}\right)\frac{T'}{T} + \frac{m}{T}\left(\frac{Iv_\parallel}{B}\right.\right.$$
$$\left.\left. + \omega R^2\right)\omega'\right]f_0 + \frac{v_\perp^2 \cos 2\zeta |\nabla\Psi|^2}{2\Omega Bv_T^2}\omega' f_0. \tag{8}$$

$\Omega = qB/m$ is the gyrofrequency and $I = RB_\phi$, where $B_\phi$ is the toroidal component of the magnetic field. The relation of the flux-surface function $N(\Psi)$ to the density is given in Eq. (12) below.

Hinton and Wong found the drift kinetic equation for $\bar{f}_1$ to be

$$v_\parallel \hat{b} \cdot \nabla \bar{f}_1 - C^l(\bar{f}_1) = -\frac{q}{T}v_\parallel \hat{b} \cdot \nabla \Phi_1 f_0$$
$$- v_\parallel f_0 \sum_{j=1}^{3} A_j(\Psi)\hat{b} \cdot \nabla \alpha_j, \tag{9}$$

where $C^l$ is the linearized collision operator. The driving terms $A_j$ are the radial gradients,

$$A_1 = \frac{N'}{N} + \frac{T'}{T}, \quad A_2 = \frac{T'}{T}, \quad A_3 = \frac{\omega'}{\omega},$$

and the coefficients $\alpha_j$ are given by

$$\alpha_1 = (m/e)[Iv_\parallel/B + \omega R^2],$$

$$\alpha_2 = \left(\frac{H}{T} - \frac{5}{2}\right)\alpha_1$$

and

$$\alpha_3 = \frac{m^2\omega}{2eT}\left[\left(\frac{Iv_\parallel}{B} + \omega R^2\right)^2 + \frac{\mu|\nabla\Psi|^2}{mB}\right].$$

References 4 and 5 used a variational method to determine the neoclassical transport coefficients for the bulk ions, so an expression for $\bar{f}_{i1}$ was not explicitly determined. Here we adopt an alternative method of solution.[8] By using a suitable form of the ion collision operator, the drift kinetic equation may be solved for $\bar{f}_{i1}$, which can then be used directly to determine the neoclassical radial fluxes and so the transport coefficients. In the next section we motivate the form of the collision operator used. This operator is of course less accurate than the exact one, but it has the advantage that it enables the kinetic equation to be solved analytically, avoiding the use of trial functions of unknown accuracy.

Finally in this summary, we consider the variation of the zeroth-order density of a species around a magnetic flux surface (see Refs. 4 and 7), which is expected to have a significant effect on the analysis here. The fluid momentum equation in the laboratory frame is

$$mn\left(\frac{\partial \mathbf{V}}{\partial t} + (\mathbf{V} \cdot \nabla)\mathbf{V}\right) = -nq\nabla\Phi - \nabla p - \nabla \cdot \boldsymbol{\pi} + \mathbf{R}$$
$$+ nq\mathbf{V} \times \mathbf{B}, \tag{10}$$

where $\mathbf{V}$ is the fluid velocity, $p$ is the pressure, $\boldsymbol{\pi}$ is the viscosity tensor, and $\mathbf{R}$ is the friction experienced by the species. As the flow velocity may be of order of the thermal speed, we cannot neglect the second term on the left. Using the zeroth-order flow velocity of Eq. (2), and noting that $\nabla \cdot \boldsymbol{\pi}$, $\mathbf{R} \ll \nabla p$, the parallel component of Eq. (10) is

$$\hat{b} \cdot \nabla\left(\ln n_0 + \frac{q}{T}\Phi_0 - \frac{m\omega^2 R^2}{2T}\right) = 0. \tag{11}$$

Integrating Eq. (11) gives

$$n_0 = N(\Psi)\exp\left(-\frac{q}{T}\tilde{\Phi}_0 + \frac{m\omega^2 R^2}{2T}\right), \tag{12}$$

where $N(\Psi)$ is an arbitrary flux function and $\tilde{\Phi}_0$ is determined by requiring charge neutrality. Wesson[7] identified $\tilde{\Phi}_0$ for the case of a trace, heavy impurity (denoted by a subscript $z$, with charge $ze$) present in a hydrogenic plasma, by assuming equal bulk ion and electron (subscript $e$) densities at all points,

$$\tilde{\Phi}_0 = \frac{T_e}{T_i + T_e}\frac{m_i\omega^2}{2e}(R^2 - R_0^2), \tag{13}$$

where $R_0$ is an arbitrary reference radius. The impurity density is then obtained from Eq. (12) by noting that the impurities feel the same potential without disturbing it, as $zn_z \ll n_i$,

$$n_z = n_{z0} \exp\left[\left(1 - \frac{T_e}{T_i + T_e} z \frac{m_i}{m_z}\right) \frac{m_z \omega^2 (R^2 - R_0^2)}{2T_z}\right], \quad (14)$$

where $n_{z0}$ is the density at the reference radius $R_0$. The impurities are therefore expected to be shifted outward in major radius by the centrifugal force, which is indeed seen experimentally.[8] Note that in the limit of very high impurity Mach number $M_z \gg 1$ all impurity ions will be localized to a disk in the outboard midplane. The effect on the lighter bulk ions is much weaker, so they undergo significant poloidal redistribution only when the bulk ion Mach number approaches 1.

## III. COLLISION OPERATOR

The impurity concentration in a tokamak is normally such that the frequencies of bulk-ion–bulk-ion collisions and bulk ion-impurity collisions are comparable, $z^2 n_z \sim n_i \gg z n_z$. Electron-ion collisions will be taken to be of higher order in $\delta$, due to the small electron-ion mass ratio, so will be neglected. Thus the linearized bulk ion collision operator in the rotating frame, $C_i^l$, will consist of two terms: $C_i^l = C_{ii}^l + C_{iz}^l$, where $C_{ii}^l$ describes bulk ion self-collisions and $C_{iz}^l$ describes bulk ion-impurity collisions.

Collisions between bulk ions may be described by the model self-collision operator of Kovrizhnykh,[10] where the first term represents pitch-angle scattering and the second momentum conservation,

$$C_{ii}^l(f_i) = \nu_D^{ii}(v', \Psi, \theta)\left(\mathcal{L}(f_i) + \frac{m_i \mathbf{v}' \cdot \mathbf{w}}{T_i} f_{i0}\right). \quad (15)$$

The angle $\theta$ measures poloidal position on a flux surface, with $\theta = 0$ at the outboard side and $f_{i0}$ is the zeroth-order Maxwellian distribution for the bulk ions. The deflection frequency is given by

$$\nu_D^{ii} = \frac{3\pi^{1/2}}{4\tau_{ii}} \frac{\phi(x) - G(x)}{x^3},$$

where $x = v'/v_{Ti}$, $\phi(x)$ is the error function, $G(x) = (\phi(x) - x\phi'(x))/2x^2$ is the Chandrasekhar function, and $\sqrt{2}\tau_{ii} = \tau_i$, with $\tau_i$ the ion-ion collision time defined by Braginskii.[11] The Lorentz operator is

$$2\mathcal{L} = \frac{\partial}{\partial \xi}(1 - \xi^2)\frac{\partial}{\partial \xi} + \frac{1}{1 - \xi^2}\frac{\partial^2}{\partial \zeta^2},$$

where the pitch-angle cosine is $\xi = v_\parallel / v'$. The constant vector $\mathbf{w}$ is chosen to ensure that momentum is conserved in the collisions,

$$\int m_i \mathbf{v}' C_{ii}(f_i) d^3 v = 0. \quad (16)$$

Typically the mass of an impurity ion present in a tokamak will be much larger than that of a bulk ion. Due to these disparate masses, the bulk ion-impurity interaction may be readily described, in a manner analagous to that for electron-ion collisions. In the limit of infinite mass ratio, the linearized Landau bulk ion-impurity collision operator reduces to

$$C_{iz}^l(f_i) = \nu_{iz}(v', \Psi, \theta)\left(\mathcal{L}(f_i) + \frac{m_i \mathbf{v}' \cdot \mathbf{V}_z}{T_i} f_{i0}\right). \quad (17)$$

The first term again describes pitch-angle scattering, where the collision frequency is $\nu_{iz} = (3\pi^{1/2}/4\tau_{iz})/x^3$ and the bulk ion-impurity collision time is $\tau_{iz} = 3(2\pi)^{3/2} m_i^{1/2} T_i^{3/2} \epsilon_0^2 / n_z z^2 e^4 \ln \Lambda$, where $\ln \Lambda$ is the Coulomb logarithm. The second term takes into account the motion of the impurities, so $\mathbf{V}_z$, the impurity fluid velocity in the rotating frame, enters. Further terms which must appear to correct for the finite mass ratio are of order $m_i/m_z$, which is of order $1/z$. They will therefore be consistently neglected throughout.

The impurity fluid velocity may be determined as follows. The impurity fluid momentum equation in the laboratory frame is given by Eq. (10) with $q = ze$. We may extract the perpendicular component of the impurity velocity in the laboratory frame by taking the cross product with $\hat{b}$, noting that Eq. (11) shows that the poloidal gradients give no contribution,

$$\mathbf{V}_{z\perp}^{(\text{lab})} = \frac{\hat{b} \times \nabla \Phi}{B} + \frac{\hat{b} \times \nabla p_z}{n_z z e B} - \frac{m_z \omega^2 \hat{b} \times \nabla R^2}{2z e B}. \quad (18)$$

We thus obtain the velocity in the rotating frame by using $\Phi = \tilde{\Phi}_0$

$$\mathbf{V}_{z\perp} = \frac{T_z}{\Omega_z m_z}\left[\frac{N_z'}{N_z} + \frac{T_z'}{T_z} + \frac{ze}{T_z}\tilde{\Phi}_0' + \frac{ze\tilde{\Phi}_0}{T_z}\frac{T_z'}{T_z} - \frac{m_z \omega^2 R^2}{2T_z}\frac{T_z'}{T_z}\right.$$
$$\left. + \frac{m_z \omega R^2}{T_z}\omega'\right]\hat{b} \times \nabla \Psi. \quad (19)$$

This expression may also be obtained by taking the velocity moment of $\tilde{f}_{z1}$.

The impurity velocity on a flux surface must be divergence free to lowest order, thus

$$\nabla \cdot (n_z \mathbf{V}_{z\perp}) = -\nabla \cdot (n_z \mathbf{V}_{z\parallel}). \quad (20)$$

As $\hat{b} \times \nabla \Psi = I\hat{b} - RB\hat{e}_\phi$,

$$\nabla \cdot (n_z \mathbf{V}_{z\perp}) = \mathbf{B} \cdot \nabla\left(\frac{In_z}{B}\frac{|\mathbf{V}_{z\perp}|}{|\nabla \Psi|}\right) = -\mathbf{B} \cdot \nabla\left(\frac{n_z V_{z\parallel}}{B}\right),$$

hence

$$V_{z\parallel} = -I\frac{|\mathbf{V}_{z\perp}|}{|\nabla \Psi|} + \frac{K(\psi)B}{n_z}. \quad (21)$$

The integration constant $K(\psi)$ completely determines the poloidal component of the impurity flow velocity. To evaluate $K(\psi)$, we retain the friction term in Eq. (10), multiply the parallel component of that equation by $B/n_z$, then take the flux-surface average. This average has its usual definition,

$$\langle A \rangle = \oint \frac{A dl_p}{B_p} \bigg/ \oint \frac{dl_p}{B_p}, \quad (22)$$

where $B_p$ is the poloidal component of the magnetic field, and $dl_p$ is an element of length poloidally around the flux surface. As $\langle B\nabla_\parallel A \rangle = 0$ for any $A$ that has poloidal periodicity, this gives

$$\left\langle \frac{BR_{z\parallel}}{n_z} \right\rangle = 0. \tag{23}$$

An explicit expression for $K$ is determined in Sec. VI. Note that we have again neglected the viscous term in Eq. (10). The requirement that the parallel viscosity is much less than the parallel impurity friction imposes the condition $\nu_{*i} \gg 1/\alpha^{1/2}z^{7/4}$, which is slightly more stringent than that first imposed in the introduction.

## IV. RADIAL TRANSPORT

The radial magnetic surface-averaged fluxes of particles, heat, and toroidal angular momentum are defined, respectively, by (see Ref. 4)

$$\Gamma = \left\langle \int d^3v \, \mathbf{v} \cdot \nabla\Psi f \right\rangle, \tag{24}$$

$$q = -\frac{5}{2}T\Gamma - \omega\Pi + \left\langle \int d^3v \left( \frac{1}{2}mv^2 + q\tilde{\Phi} \right) \mathbf{v} \cdot \nabla\Psi f \right\rangle, \tag{25}$$

and

$$\Pi = \left\langle \int d^3v \, mR v_\phi \mathbf{v} \cdot \nabla\Psi f \right\rangle, \tag{26}$$

where $v_\phi = \mathbf{v}' \cdot \hat{e}_\phi$.

Hinton and Wong showed that the leading term in the radial transport is of order $\delta^2$, so $f_2$ would be required to evaluate it using the expressions above. A simpler approach is to calculate the transport using flux-friction relations, obtained by flux-surface averaging appropriate velocity moments of the Fokker-Planck equation. This process is detailed in Ref. 4 and the resulting expressions for the leading order contributions to the bulk ion fluxes, in terms of collisional moments of $f_{i1}$, are

$$\Gamma_2 = -\frac{1}{e} \left\langle \int d^3v \, m_i R v_\phi C_i^l(f_{i1}) \right\rangle, \tag{27}$$

$$q_2 = -\frac{5}{2}T_i\Gamma_2 - \omega\Pi_2 - \frac{m_i}{e}\left\langle \int d^3v \, R v_\phi \left( \frac{1}{2}m_i v^2 \right.\right.$$
$$\left.\left. + e\tilde{\Phi}_0 \right) C_i^l(f_{i1}) \right\rangle, \tag{28}$$

and

$$\Pi_2 = -\frac{m_i}{e} \left\langle \int d^3v \, \frac{1}{2}m_i R^2 v_\phi^2 C_i^l(f_{i1}) \right\rangle. \tag{29}$$

We will drop the subscript 2 for the remainder of this paper. As $f_1 = \bar{f}_1 + \tilde{f}_1$ we may express each flux as the sum of classical (denoted by a tilde) and neoclassical parts (denoted by a bar and dependent only on the gyroaveraged distribution function).

$$\tilde{\Gamma} = -\frac{m_i}{e} \left\langle \int d^3v \, R(\hat{e}_\phi \cdot \hat{e}_2) v_\perp \sin\zeta C_i^l(\tilde{f}_{i1}) \right\rangle, \tag{30}$$

$$\tilde{q} = -\frac{m_i}{e} \left\langle \int d^3v \, R(\hat{e}_\phi \cdot \hat{e}_2) v_\perp \sin\zeta \left( H - \frac{5}{2}T_i \right) C_i^l(\tilde{f}_{i1}) \right\rangle, \tag{31}$$

$$\tilde{\Pi} = -\frac{m_i}{e} \left\langle \int d^3v \, \frac{m_i}{2} R^2 [2(\omega R + v_\parallel \hat{b} \cdot \hat{e}_\phi) v_\perp (\hat{e}_\phi \cdot \hat{e}_2) \sin\zeta \right.$$
$$\left. - (v_\perp^2/2)(\hat{e}_\phi \cdot \hat{e}_2)^2 \cos 2\zeta] C_i^l(\tilde{f}_{i1}) \right\rangle, \tag{32}$$

$$\bar{\Gamma} = -\left\langle \int d^3v \, \alpha_1 C_i^l(\bar{f}_{i1}) \right\rangle, \tag{33}$$

$$\bar{q} = -\left\langle \int d^3v \, T_i \alpha_2 C_i^l(\bar{f}_{i1}) \right\rangle, \tag{34}$$

and

$$\bar{\Pi} = -\left\langle \int d^3v \, \frac{T_i}{\omega} \alpha_3 C_i^l(\bar{f}_{i1}) \right\rangle. \tag{35}$$

Note that $\hat{e}_\phi \cdot \hat{e}_2 = -|\nabla\Psi|/BR$ and $|\nabla\Psi| = RB_p$, where the poloidal field satisfies $B_p^2 = B^2 - I^2/R^2$.

## V. CLASSICAL FLUXES

An expression for $\tilde{f}_1$ was given in Sec. II and this may be used to directly evaluate the classical fluxes for arbitrary rotation speed. We separate the contributions arising from bulk-ion–bulk-ion and bulk ion-impurity collisions for clarity, so, for example, $\tilde{\Gamma} = \tilde{\Gamma}^{ii} + \tilde{\Gamma}^{iz}$, where

$$\tilde{\Gamma}^{ii} = -\frac{m_i}{e} \left\langle \int d^3v \, R(\hat{e}_\phi \cdot \hat{e}_2) v_\perp \sin\zeta C_{ii}^l(\tilde{f}_{i1}) \right\rangle. \tag{36}$$

The bulk-bulk contributions to the fluxes may be evaluated in the manner presented by Braginskii,[11] using the exact ion-ion collision operator of Landau, rather than the model operator discussed in Sec. III. So,

$$C_{ii}^l(f_{i1}) = C_{ii}(f_{i1}, f_{i0}) + C_{ii}(f_{i0}, f_{i1}) \tag{37}$$

and the velocity integrals in Eqs. (30)–(32) may be identified as linear combinations of Braginskii matrix elements of the collision operator (see Ref. 11). Noting that evaluation of $\tilde{\Pi}^{ii}$ is simplified by remembering that energy conservation requires $\int d^3v \, v^2 C_{ii}^l(v^2 f_{i0}) = 0$ and that,[5] for an arbitrary unit vector $\mathbf{a}$, $\int d^3v (\mathbf{a} \cdot \mathbf{v})^2 C_{ii}^l[(\mathbf{a} \cdot \mathbf{v})^2 f_{i0}] = -\frac{2}{5}\frac{n_i}{\tau_i}v_{Ti}^4$, the bulk-bulk contributions are found to be

$$\tilde{\Gamma}^{ii} = 0, \tag{38}$$

$$\frac{\tilde{q}^{ii}}{T_i} = -\left\langle \frac{p_i |\nabla\Psi|^2}{m_i \Omega_i^2} \frac{2}{\tau_i} \right\rangle \frac{T_i'}{T_i}, \tag{39}$$

and

$$\tilde{\Pi}^{ii} = -\left\langle \frac{p_i|\nabla\Psi|^2}{\Omega_i^2} \frac{3}{10\tau_i}\left(3\frac{I^2}{B^2}+R^2\right)\right\rangle \omega'. \tag{40}$$

Equations (38)–(40) coincide with the fluxes determined in Ref. 4 in the case of a pure plasma.

The contributions to the fluxes from bulk-impurity collisions will be evaluated using the operator described in Sec. III. Firstly, we recognize that the gyrophase dependence of Eqs. (30)–(32) is such that the term proportional to $V_{z\parallel}$ in the bulk-impurity collision operator gives no contribution to the integrals. Thus, for example, the contribution to the particle flux is

$$\tilde{\Gamma}^{iz} = -\left\langle \frac{|\nabla\Psi|}{\Omega_i}\int d^3v v_\perp \sin\zeta \nu_{iz}\left\{\mathcal{L}(\tilde{f}_{i1})\right.\right.$$
$$\left.\left. + \frac{m_i}{T_i}\mathbf{v}_\perp\cdot\mathbf{V}_{z\perp}f_{i0}\right\}\right\rangle, \tag{41}$$

where the form of $\mathbf{V}_{z\perp}$ may be inserted from Eq. (19). Reference 12 shows that $(T_i-T_z)/T_i \sim \delta/z\nu_{*i}$, which is small with the orderings present here, so the impurity temperature may be taken to be equilibrated with the bulk ion temperature. Thus we neglect differences between the bulk ion and impurity temperature gradients in the following.

The action of $\mathcal{L}$ on the velocity components present in $\tilde{f}_{i1}$ is $\mathcal{L}(v_\perp\sin\zeta)=-v_\perp\sin\zeta$, $\mathcal{L}(v_\parallel v_\perp\sin\zeta)=-3v_\parallel v_\perp\sin\zeta$, and $\mathcal{L}(v_\perp^2\cos 2\zeta)=-3v_\perp^2\cos 2\zeta$. Denoting the velocity components by $v_n = \mathbf{v}'\cdot\hat{e}_n$, we must evaluate velocity integrals of the form $\int d^3v\nu_{iz}(v^2)^m v_2^2 f_{i0}$, where $m$ is 0, 1, or 2, to determine the contributions to the particle and heat fluxes, whilst the momentum flux also requires $\int d^3v\nu_{iz}v_3^2 v_2^2 f_{i0}$ and $\int d^3v\nu_{iz}(v_\perp^2\cos 2\zeta)^2 f_{i0}$. After performing the integral over gyrophase, the remaining integral in each case may be rewritten using the variables $(v,\alpha)$, where $0<v<\infty$ and $-\pi/2<\alpha<\pi/2$, and evaluated. Hence, neglecting terms of order $1/z$, we find

$$\tilde{\Gamma}^{iz} = -\left\langle \frac{p_i|\nabla\Psi|^2}{m_i\Omega_i^2}\frac{G}{\tau_{iz}}\right\rangle, \tag{42}$$

$$\frac{\tilde{q}^{iz}}{T_i} = -\left\langle \frac{p_i|\nabla\Psi|^2}{m_i\Omega_i^2}\left[\frac{e\tilde{\Phi}_0}{T_i}-\frac{m_i\omega^2R^2}{2T_i}-\frac{3}{2}\right]\frac{G}{\tau_{iz}}\right\rangle$$
$$-\left\langle \frac{p_i|\nabla\Psi|^2}{m_i\Omega_i^2}\frac{1}{\tau_{iz}}\right\rangle\frac{T_i'}{T_i}, \tag{43}$$

$$\tilde{\Pi}^{iz} = -\left\langle \frac{p_i|\nabla\Psi|^2}{m_i\Omega_i^2}m_i\omega R^2\frac{G}{\tau_{iz}}\right\rangle - \left\langle \frac{p_i|\nabla\Psi|^2}{\Omega_i^2}\frac{3}{10\tau_{iz}}\left[3\frac{I^2}{B^2}\right.\right.$$
$$\left.\left. + R^2\right]\right\rangle \omega', \tag{44}$$

where $G$ defines the following combination of driving terms:

$$G = \frac{N_i'}{N} - \frac{1}{2}\frac{T_i'}{T_i} - \left(m_i - \frac{m_z}{z}\right)\frac{\omega^2R^2}{2T_i}\left\{\frac{T_i'}{T_i}-2\frac{\omega'}{\omega}\right\}. \tag{45}$$

The bulk ion-impurity collision time $\tau_{iz}$ is inversely proportional to the impurity density, which, by Eq. (14), will be pushed towards the outboard side of a flux surface. Thus the

flux-surface averages in Eqs. (42)–(44) will be primarily determined by conditions at the outboard side, and we may expect the classical angular momentum transport $\tilde{\Pi}/|\nabla\Psi|$ to be enhanced due to the bulk-impurity contribution by the ratio of $R^2/B^2$ at the outboard side to its flux-surface average. This enhancement may be understood in the following way. The classical transport is collisional diffusion with a step size of order of the ion gyroradius. The angular momentum $m_i\omega R^2$ carried by a particle and the step size are larger at the low-field outboard side, which is where most of the collisions causing the radial transport occur. The enhancement will be most significant in a spherical tokamak, where $R^2/B^2$ varies substantially over a flux surface.

## VI. NEOCLASSICAL FLUXES IN A PLASMA WITH SUBSONIC ROTATION

In this section we restrict the analysis to subsonic rotation of the bulk plasma. Specifically, we take

$$M_i^2 = \frac{m_i\omega^2R^2}{2T_i} \sim \frac{1}{z} \ll 1. \tag{46}$$

With this ordering the impurity Mach number is of order unity, thus strong poloidal redistribution of impurities may be expected from Eq. (14), but $n_i$ will be approximately constant around a flux surface. Electrostatic trapping of bulk ions is negligible as Eq. (13) shows that $e\tilde{\Phi}_0 \sim T_i/z$. The velocity $v$ will be an approximate constant of motion, so we may use it to replace the energy variable $H$. Thus the independent variables now are $(v,\lambda,\sigma,\psi)$, where $\lambda=v_\perp^2/(v^2B)$ and $\sigma=v_\parallel/|v_\parallel|$, and the Lorentz operator may be written as

$$\mathcal{L} = \frac{2\xi}{B}\frac{\partial}{\partial\lambda}\lambda\xi\frac{\partial}{\partial\lambda}. \tag{47}$$

Finally, noting that terms of order $M_i^2A_3$ must be retained, the expression for the parallel impurity velocity, Eq. (21), reduces to

$$V_{z\parallel} = -\frac{I}{B}\left(\frac{\partial\tilde{\Phi}_0}{\partial\psi}+\frac{m_z\omega R^2}{ze}A_3\right)+\frac{K(\psi)B}{n_z}. \tag{48}$$

Equation (9) must now be solved for $\bar{f}_{i1}$ in the "banana regime" of low collisionality. (For the remainder of this section we shall drop the bar and subscript $i$.) To do so, we perform a subsidary expansion of $f_1$ in the small ratio of the ion collision frequency to the typical ion bounce frequency. With a bracketed superscript denoting the order of expansion, the zeroth-order equation gives

$$f_1^{(0)} = F + g, \tag{49}$$

where

$$F = \left(-\frac{e}{T}\Phi_1 - \sum_{j=1}^{3}A_j(\Psi)\alpha_j\right)f_0 \tag{50}$$

and $g$ is a constant along a field line, thus is a function only of $v$, $\lambda$, $\sigma$, and $\Psi$. Equation (49) is constrained by the first-order equation,

$$v_{\parallel}\nabla_{\parallel}f_1^{(1)} = C_i^l(f_1^{(0)}). \tag{51}$$

Here we use the gyroaveraged form of the collision operator described in Sec. III,

$$C_i^l(f_1^{(0)}) = \nu_i \mathcal{L}(f_1^{(0)}) + \frac{m_i v_{\parallel}}{T_i}(\nu_{ii}w_{\parallel} + \nu_{iz}V_{z\parallel})f_{i0}, \tag{52}$$

where $\nu_i = \nu_{ii} + \nu_{iz}$.

It is convenient to decompose the driving term $F$ into Legendre polynomials $P_n$ so

$$F = \sum_{n=0}^{2} F_n(v,\psi,\theta)P_n(\xi), $$

as the action of the Lorentz operator on these polynomials is simple, and to introduce a generalized notation, which essentially extends the usual flux-surface average to include the trapped domain,

$$\langle A \rangle = \sum_{\sigma} \int_{-\theta_b}^{\theta_b} \frac{d\theta}{\mathbf{B}\cdot\nabla\theta} \Big/ 2\int_{-\pi}^{\pi} \frac{d\theta}{\mathbf{B}\cdot\nabla\theta}, \tag{53}$$

where $\pm\theta_b$ defines the bounce points of the particle orbit, which are $\pm\pi$ for passing particles.

Equation (51) is solved for $\partial g/\partial\lambda$ in the passing regime in the usual way, by multiplying by $B/v_{\parallel}$ and taking the flux-surface average. This gives

$$\left\langle \frac{B\nu_i}{v_{\parallel}}\mathcal{L}(g+F) + \frac{m_i B}{T_i}(\nu_{ii}w_{\parallel} + \nu_{iz}V_{z\parallel})f_{i0} \right\rangle = 0. \tag{54}$$

Trapped particles are those with $\lambda_c < \lambda < \lambda_{\max}$, where the trapped-passing boundary is marked by $\lambda_c = 1/B(\theta=\pi) = 1/B_{\max}$, and the maximum value of $\lambda$ permissible on the flux surface is $\lambda_{\max} = 1/B(\theta=0) = 1/B_{\min}$. In the trapped region, $\partial g/\partial\lambda$ is determined by integrating Eq. (51) over a complete orbit, giving

$$\oint \nu_i \mathcal{L}(g+F_2 P_2) dt = 0. \tag{55}$$

The flux in velocity space should be continuous across the trapped-passing boundary, which implies

$$\sum_{\sigma} \frac{\partial g}{\partial\lambda}\bigg|_{\lambda=\lambda_c^-} = \sum_{\sigma} \frac{\partial g}{\partial\lambda}\bigg|_{\lambda=\lambda_c^+}.$$

Upon matching the solutions we thus obtain

$$\frac{\partial g}{\partial\lambda} = \frac{\sigma H(\lambda_c - \lambda)}{2\langle \nu_i\sqrt{1-\lambda B}\rangle}\left\langle B\nu_i F_1 - \frac{m_i v B}{T_i}(\nu_{ii}w_{\parallel} + \nu_{iz}V_{z\parallel})f_{i0} \right\rangle$$
$$+ \frac{3}{2}\frac{\langle B\nu_i F_2\sqrt{1-\lambda B}\rangle}{\langle \nu_i\sqrt{1-\lambda B}\rangle}, \tag{56}$$

where $H$ is the Heaviside step function.

To evaluate the fluxes we require $K$, the remaining unknown in $V_{z\parallel}$ [see Eq. (21)]. This may be obtained, as described by Eq. (23), by considering the parallel impurity-bulk ion friction $R_{z\parallel} = -R_{iz\parallel} = -\int d^3v\, m_i v_{\parallel}C_{iz}^l(f_{i1})$. To lowest order, using Eq. (52),
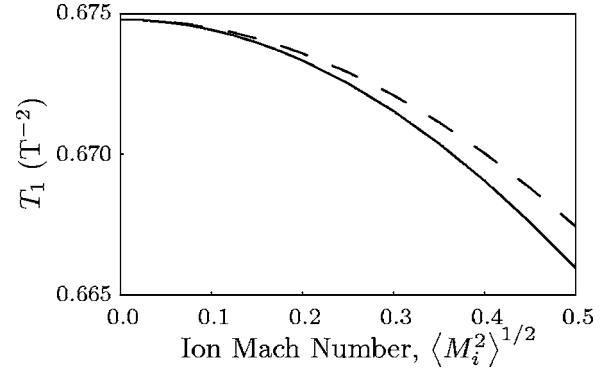


FIG. 1. The true (solid) and approximated (dashed) values of $T_1$ as a function of the bulk ion Mach number $\langle M_i^2\rangle^{1/2}$ for $\langle Z_{\mathrm{eff}}\rangle = 2$ and $\varepsilon \sim 0.32$.

$$R_{zi\parallel} = \frac{3\sqrt{\pi}}{4\tau_{iz}}\int \frac{m_i v_{\parallel}}{x^3}\left(F + g - \frac{m_i v_{\parallel}}{T_i}V_{z\parallel}f_{i0}\right)d^3v, \tag{57}$$

where we have used the self-adjoint property of $\mathcal{L}$ to write $v_{\parallel}\mathcal{L}(f_1^{(0)}) = -v_{\parallel}f_1^{(0)}$ under the velocity integral. Thus

$$R_{zi\parallel} = \frac{m_i n_i B}{\tau_{iz}}\left(u - \frac{K}{n_z}\right) + \frac{p_i}{\Omega_i \tau_{iz}L_{\perp}}, \tag{58}$$

where the perpendicular length scale is defined as

$$\frac{1}{L_{\perp}} = -I\left[A_1 - \frac{3}{2}A_2 + 2\left(M_i^2 - \frac{T_z}{T_i}\frac{M_z^2}{z}\right)A_3\right] \tag{59}$$

and

$$u = -\frac{3\pi^{3/2}}{2n_i}v_{Ti}^4\int_0^{\infty}dx\int_0^{\lambda_c}\lambda\frac{\partial g_{\mathrm{odd}}}{\partial\lambda}d\lambda, \tag{60}$$

where $g_{\mathrm{odd}}$ is that part of $g$ which is odd with respect to $\sigma$. Note that $u$ is a flux-surface function and we have neglected the small term $(e/T_i)(\partial\tilde{\phi}_0/\partial\Psi)$.

Due to the different velocity dependencies of $\nu_{ii}$ and $\nu_{iz}$, the integral defining $u$ cannot be evaluated analytically, except in the limits $Z_{\mathrm{eff}}\to 1$ and $Z_{\mathrm{eff}}\to\infty$, where the effective plasma charge $Z_{\mathrm{eff}} = 1 + \alpha$. In order to interpolate between these limits, we modify the velocity dependence of the integrand in Eq. (60) slightly, by taking $\nu_{ii}$ and $\nu_{iz}$ to depend in the same way on velocity. This modification is, of course, not rigorously justified, but as a linear combination of $\nu_{ii}$ and $\nu_{iz}$ appears both in the numerator and denominator of Eq. (56), it does not make a significant quantitative difference once the integration is carried out. This is demonstrated in Fig. 1, which shows the true and approximated values of a typical term $T_1$ in Eq. (60) as a function of bulk ion Mach number $\langle M_i^2\rangle^{1/2}$, where

$$T_1 = \int_0^{\infty}dx\, x e^{-x^2}\int_0^{\lambda_c}\frac{\langle\nu_i\rangle}{\langle\nu_i\sqrt{1-\lambda B}\rangle}\lambda\, d\lambda.$$

(Further details of how such a term may be evaluated are given in the discussion of numerical modeling at the end of Sec. VII.) The agreement was seen to be maintained across the relevant ranges of toroidal rotation velocities, $\langle Z_{\mathrm{eff}}\rangle$, and aspect ratio. Furthermore, this approximation is exact in the

limits $Z_{\text{eff}} \to 1$ and $Z_{\text{eff}} \to \infty$, between which we wish to interpolate. Thus we take

$$\frac{\nu_{iz}}{\nu_{ii}} \approx \frac{\tau_{ii}}{\tau_{iz}} = Z_{\text{eff}} - 1, \tag{61}$$

so

$$\nu_i = \nu_{ii}\left(1 + \frac{\nu_{iz}}{\nu_{ii}}\right) \approx \nu_{ii}Z_{\text{eff}}.$$

In this approximation,

$$u = \frac{f_c}{\langle B^2 \rangle}\left[ \frac{IT_i}{e}\left(A_1 - \frac{3}{2}A_2 + 2\frac{\langle Z_{\text{eff}}M_i^2 \rangle}{\langle Z_{\text{eff}} \rangle}A_3\right) \right. $$
$$\left. + \frac{\langle Bw_\parallel + (Z_{\text{eff}} - 1)BV_{z\parallel} \rangle}{\langle Z_{\text{eff}} \rangle} \right], \tag{62}$$

where the "effective fraction" of circulating particles $f_c$ is a generalization of that defined in Ref. 13,

$$f_c = \frac{3}{4}\langle B^2 \rangle \langle Z_{\text{eff}} \rangle \int_0^{\lambda_c} \frac{\lambda d\lambda}{\langle Z_{\text{eff}}\sqrt{1 - \lambda B} \rangle}. \tag{63}$$

The quantity $\langle w_\parallel B \rangle$ appears in $u$. This may be determined by noting that the momentum conservation requires $R_{ii\parallel} = 0$, then repeating the steps taken above for $R_{z\parallel}$, now using $C_{ii}^l$ given by Eq. (52).

Thus, the constant $K(\Psi)$ in Eq. (21) is determined explicitly upon substituting Eqs. (58) and (62) into Eq. (23),

$$K = \frac{T_i}{e}\frac{\{(1/L_1) - (f_c f_t/\langle Z_{\text{eff}} \rangle)[(3/2) - (\eta_2/\eta_1)]IA_2\}}{\langle (1 - f_c\zeta)(B^2/n_z) \rangle}, \tag{64}$$

where $f_t = 1 - f_c$, $\zeta = Z_{\text{eff}}/\langle Z_{\text{eff}} \rangle$, $L_1^{-1} = \langle (1 - f_c\zeta)/L_\perp \rangle$, $\eta_1 = \sqrt{2} - \ln(1 + \sqrt{2})$, and $\eta_2 = (5/2)\eta_1 - (1/\sqrt{2})$.

We may now proceed to determine the neoclassical fluxes.[14] The following normalized quantities are useful: $n = n_z/\langle n_z \rangle$ and $r^2 = R^2/R_0^2$, where $R_0^2 = \langle R^2 \rangle$, $b^2 = B^2/B_0^2$, and $B_0^2 = \langle B^2 \rangle$ now.

The particle flux, given by Eq. (33), is driven by the toroidal collisional friction experienced by the ions and may be rewritten as

$$\bar{\Gamma} = -\left\langle \frac{I}{eB}R_{iz\parallel} \right\rangle, \tag{65}$$

by noting $\int d^3v \, \omega R^2 C_{ii}^l(\bar{f}_1) = 0$ and $R_{ii\parallel} = 0$. Thus, using Eqs. (58) and (62), we find

$$\bar{\Gamma} = \frac{Ip_i\langle \tau_{iz}^{-1} \rangle}{m_i\langle \Omega_i^2 \rangle}\left[ \left\langle \left(\frac{n}{b^2} - 1\right)\frac{1}{L_\perp} \right\rangle + \left(\left\langle \frac{b^2}{n} \right\rangle - 1\right)\frac{e\langle B^2 \rangle}{T_i\langle n_z \rangle}K \right]. \tag{66}$$

As $n_i$ is approximately constant on a flux surface, $p_i$ may be taken outside the flux-surface averages here.

The heat flux is given by Eq. (34), which, in the case of subsonic rotation where $H \approx m_i v^2/2$, becomes

$$\bar{q} = -\left\langle \frac{IT_i}{eB}\int m_iv_\parallel\left(x^2 - \frac{5}{2}\right)C_i^l(f_1)d^3v \right\rangle$$
$$= -\left\langle \frac{IT_i}{eB}\int m_iv_\parallel x^2 C_i^l(f_1)d^3v \right\rangle + \frac{5T_i}{2}\left\langle \frac{I}{eB}R_{iz\parallel} \right\rangle. \tag{67}$$

Only terms in $C_i^l(f_1)$ which are odd with respect to $v_\parallel$ will contribute to the first term. This also occurred in the evaluation of $R_{iz\parallel}$, thus, upon performing the integral over $x$, we may again use $u$ and $R_{ii\parallel} = 0$ to write this first term as $T_i\bar{\Gamma}$ plus an additional contribution proportional to the temperature gradient $A_2$. Hence the heat flux takes the form

$$\bar{q} = -\frac{3}{2}T_i\bar{\Gamma} - \frac{p_iT_iI^2A_2}{m_i\hat{\Omega}_i^2}\left\langle \left\{\frac{1}{\tau_{iz}} + \frac{[(\eta_2/\eta_1) - (1/4)]}{\sqrt{2}\tau_{ii}}\right\} \right.$$
$$\left. \times \left(\frac{1}{b^2} - f_c\right) \right\rangle. \tag{68}$$

The angular momentum flux is given by Eq. (35),

$$\bar{\Pi} = -\frac{T_i}{\omega}\left\langle \int \alpha_3\left[ \nu_i\mathcal{L}(F + g) + \frac{m_iv_\parallel}{T_i}(\nu_{ii}w_\parallel \right.\right.$$
$$\left.\left. + \nu_{iz}V_{z\parallel})f_{i0} \right]d^3v \right\rangle. \tag{69}$$

The terms in this equation may be divided into two groups, corresponding to the occurence of terms in $\alpha_3$ which are odd and even with respect to $\sigma$.

Odd terms in $\alpha_3$ combine with the terms in the collision operator containing $F_1$, $g_{\text{odd}}$, $w_\parallel$, and $V_{z\parallel}$, to give a contribution, $\bar{\Pi}^{(1)}$, involving the total parallel ion friction $R_{i\parallel} = R_{ii\parallel} + R_{iz\parallel}$,

$$\bar{\Pi}^{(1)} = -\left\langle \frac{I}{eB}m_i\omega R^2 R_{i\parallel} \right\rangle. \tag{70}$$

As $R_{ii\parallel} = 0$, consideration of Eq. (65) gives

$$\bar{\Pi}^{(1)} = \frac{Ip_i\omega R_0^2\langle \tau_{iz}^{-1} \rangle}{\langle \Omega_i^2 \rangle}\left[ \left\langle \frac{nr^2}{b^2}\frac{1}{L_\perp} \right\rangle - \langle nr^2 \rangle\left\langle \frac{1}{L_\perp} \right\rangle \right.$$
$$\left. + \left(\langle nr^2 \rangle\left\langle \frac{b^2}{n} \right\rangle - 1\right)\frac{e\langle B^2 \rangle}{T_i\langle n_z \rangle}K \right]. \tag{71}$$

The remaining contribution to Eq. (69), denoted as $\bar{\Pi}^{(2)}$, is formed by the even terms in $\alpha_3$ combining with terms in the collision operator containing $F_2$ and the part of $g$ which is even with respect to $\sigma$, $g_{\text{even}}$. An integral over $\lambda$, analogous to that seen in Eq. (60), is required to evaluate the terms containing $g_{\text{even}}$. We therefore apply the same approximation $\nu_i \approx \nu_{ii}Z_{\text{eff}}$ in order to interpolate the contribution between the exact limits $Z_{\text{eff}} \to 1$ and $Z_{\text{eff}} \to \infty$. For these terms it is also useful to note, recalling the generalized flux-surface average from Eq. (53), that for arbitrary functions $h(\theta)$ and $k(\lambda, \theta)$,

$$\left\langle h(\theta) \int_0^{B^{-1}(\theta)} k(\lambda, \theta)d\lambda \right\rangle$$

$$= \frac{\int_{-\pi}^{\pi} (hd\theta/\mathbf{B}\cdot\nabla\theta)\left(\int_0^{B^{-1}} kd\lambda\right)}{\int_{-\pi}^{\pi} d\theta/\mathbf{B}\cdot\nabla\theta}$$

$$= \frac{\int_0^{B_{\min}^{-1}} d\lambda \left[\int_{-\theta_b}^{\theta_b} (hkd\theta/\mathbf{B}\cdot\nabla\theta)\right]}{\int_{-\pi}^{\pi} d\theta/\mathbf{B}\cdot\nabla\theta}$$

$$= \int_0^{B_{\min}^{-1}} \langle hk\rangle d\lambda.$$

Thus, with the first contribution arising from terms containing $g_{\text{even}}$ and the second from those containing $F_2$, we find

$$\overline{\Pi}^{(2)} = \frac{2}{5}\frac{p_i\omega R_0^4 B_0^2}{\langle\Omega_i^2\rangle}\left[\frac{15}{4}B_0^2\int_0^{B_{\min}^{-1}}\left\langle\frac{\beta}{\tau'}\right\rangle\frac{\langle Z_{\text{eff}}\beta\rangle}{\langle Z_{\text{eff}}\sqrt{1-\lambda B}\rangle}\lambda d\lambda \right.$$
$$\left. -\left\langle\frac{r^4}{\tau'}\left(\frac{B_\phi^2 - B_p^2/2}{B^2}\right)^2\right\rangle\right]A_3, \tag{72}$$

where $\tau'^{-1} = \tau_i^{-1} + \tau_{iz}^{-1}$ and we have denoted by $\beta$ the repeated factor $(r^2/b)[(B_\phi^2 - B_p^2/2)/B_0^2]\sqrt{1-\lambda B}$.

## VII. TRANSPORT COEFFICIENTS FOR A PLASMA WITH SUBSONIC ROTATION

The radial fluxes may be conveniently summarized by the transport matrix $L$ which relates the three fluxes to the three driving terms defined by the radial gradients $A_1$, $A_2$, and $A_3$. Thus, we write

$$\begin{pmatrix}\langle\mathbf{\Gamma}_i\cdot\nabla\Psi\rangle \\ \langle\mathbf{q}_i\cdot\nabla\Psi\rangle_n \\ \langle R\hat{e}_\phi\cdot\boldsymbol{\pi}\cdot\nabla\Psi\rangle_n\end{pmatrix} = -\begin{pmatrix}L_{11} & L_{12} & L_{13} \\ L_{21} & L_{22} & L_{23} \\ L_{31} & L_{32} & L_{33}\end{pmatrix}\begin{pmatrix}A_1 \\ A_2 \\ A_3\end{pmatrix},$$

where the normalized fluxes $\langle\mathbf{q}_i\cdot\nabla\Psi\rangle_n = \langle\mathbf{q}_i\cdot\nabla\Psi\rangle/T_i$ and $\langle R\hat{e}_\phi\cdot\boldsymbol{\pi}\cdot\nabla\Psi\rangle_n = \langle R\hat{e}_\phi\cdot\boldsymbol{\pi}\cdot\nabla\Psi\rangle/m_i\omega R_0^2$.

Defining the constant $A = p_i I^2\langle\tau_{iz}^{-1}\rangle/m_i\langle\Omega_i^2\rangle$, the elements of the transport matrix $L_{ij}$ are given by $Al_{ij}$, where each transport coefficient $l_{ij}$ is the sum of classical $\tilde{l}_{ij}$ and neoclassical $\overline{l}_{ij}$ parts, so $L_{ij} = \tilde{L}_{ij} + \overline{L}_{ij}$. Considering the form of $\overline{\Pi}_2$ we write $\overline{l}_{33}$ as the sum $\overline{l}_{33}^{(1)} + \overline{l}_{33}^{(2)}$, where the contribution $\overline{l}_{33}^{(1)}$ is taken from $\overline{\Pi}_2^{(1)}$ and $\overline{l}_{33}^{(2)}$ from $\overline{\Pi}_2^{(2)}$. Note that $\overline{L}_{33}$ is proportional to the value typically quoted as the neoclassical toroidal viscosity. Taking $T_i = T_z$, as discussed in Sec. IV, explicit expressions for the neoclassical coefficients are

$$\overline{l}_{11} = \left\langle\frac{n}{b^2}\right\rangle - 1 + f_t\frac{\langle b^2/n\rangle - 1}{\langle(1-f_c\zeta)(b^2/n)\rangle}, \tag{73}$$

$$\overline{l}_{12} = -\frac{3}{2}\overline{l}_{11} + \left(\frac{3}{2} - \frac{\eta_2}{\eta_1}\right)\frac{f_cf_t}{\langle Z_{\text{eff}}\rangle}\frac{\langle b^2/n\rangle - 1}{\langle(1-f_c\zeta)(b^2/n)\rangle}, \tag{74}$$

$$\overline{l}_{13} = 2\left\langle M_i^2 - \frac{M_z^2}{z}\right\rangle\overline{l}_{31}, \tag{75}$$

$$\overline{l}_{21} = -\frac{3}{2}\overline{l}_{11}, \tag{76}$$

$$\overline{l}_{22} = -\frac{3}{2}\overline{l}_{12} + \frac{1}{\langle\tau_{iz}^{-1}\rangle}\left\langle\left(\frac{1}{\tau_{iz}} + \frac{[(\eta_2/\eta_1) - (1/4)]}{\sqrt{2}\tau_{ii}}\right)\right.$$
$$\left.\times\left(\frac{1}{b^2} - f_c\right)\right\rangle, \tag{77}$$

$$\overline{l}_{23} = -\frac{3}{2}\overline{l}_{13}, \tag{78}$$

$$\overline{l}_{31} = \left\langle\frac{nr^2}{b^2}\right\rangle - f_c\langle nr^2\rangle - f_t\frac{1 - f_c\langle nr^2\rangle\langle(b^2/n)\zeta\rangle}{\langle(1-f_c\zeta)(b^2/n)\rangle}, \tag{79}$$

$$\overline{l}_{32} = -\frac{3}{2}\overline{l}_{31} + \left(\frac{3}{2} - \frac{\eta_2}{\eta_1}\right)\frac{f_cf_t}{\langle Z_{\text{eff}}\rangle}\frac{\langle(b^2/n)\rangle\langle nr^2\rangle - 1}{\langle(1-f_c\zeta)(b^2/n)\rangle}, \tag{80}$$

$$\overline{l}_{33}^{(1)} = 2\left\langle M_i^2 - \frac{M_z^2}{z}\right\rangle\left[\left\langle\frac{nr^4}{b^2}\right\rangle - f_c\langle nr^2\rangle\langle\zeta r^2\rangle\right.$$
$$\left. - (1 - f_c\langle\zeta r^2\rangle)\frac{(1 - f_c\langle nr^2\rangle\langle(b^2/n)\zeta\rangle)}{\langle(1-f_c\zeta)(b^2/n)\rangle}\right], \tag{81}$$

and

$$\overline{l}_{33}^{(2)} = -\frac{2}{5}\frac{R_0^2 B_0^2}{I^2}\left[\frac{15}{4}B_0^2\int_0^{B_{\min}^{-1}}\left\langle\frac{\beta}{\tau'}\right\rangle\frac{\langle Z_{\text{eff}}\beta\rangle}{\langle Z_{\text{eff}}\sqrt{1-\lambda B}\rangle}\lambda d\lambda \right.$$
$$\left. -\left\langle\frac{r^4}{\tau'}\left(\frac{B_\phi^2 - B_p^2/2}{B^2}\right)^2\right\rangle\right]. \tag{82}$$

They are valid for arbitrary flux-surface geometry and impurity distribution. In the case of infinite aspect ratio, $n_z$, and thus $Z_{\text{eff}}$ are constant around a flux surface and the expressions for the neoclassical transport coefficients become exactly zero as expected.

### A. Pure plasma, $Z_{\text{eff}} = 1$

In the case of a pure plasma, $Z_{\text{eff}} = 1$ and $\tau_{iz} \to \infty$. The classical fluxes therefore reduce to $\tilde{\Gamma}^{ii}$, $\tilde{q}^{ii}$, and $\tilde{\Pi}^{ii}$, as given by Eqs. (38)–(40) and in agreement with Ref. 4. Of the neoclassical fluxes, only $\overline{l}_{22}$ and $\overline{l}_{33}^{(2)}$ are nonzero.

Hinton and Wong[4] determined the neoclassical contribution to $L_{33}$ for a pure plasma, with arbitrary rotation velocity, in the limit of large aspect ratio. To take the same limit of $A\overline{l}_{33}^{(2)}$, one notes that $R_0$ is equal to the radius of the magnetic axis to lowest order in $\varepsilon$ and takes $B = B_0/(1 + \varepsilon\cos\theta)$, where $\varepsilon = a/R_0$ is the inverse aspect ratio and $a$ is the minor radius. Thus $I \approx R_0 B_0$ and adopting the same form for the ion density, $n_i = \overline{n}_i(\Psi)\exp(X\varepsilon\cos\theta)$, where $\overline{n}_i(\Psi)$ is an arbitrary function and $X = m_i\omega^2 R_0^2/T_e + T_i$ is small, rather than assuming $n_i$ is constant around a flux surface, we recover Hinton and Wong's result,

$$\bar{L}_{33} = \frac{1}{5}\left(\frac{m}{e}\omega R_0^2\right)^2 \frac{\bar{n}_i^2}{n_i \tau_i}\varepsilon^2. \tag{83}$$

## B. Impure plasma, $Z_{\rm eff} - 1 \sim O(1)$

The expressions for the neoclassical transport coefficients were derived accounting for both bulk-ion–bulk-ion and bulk ion-impurity collisions that is $Z_{\rm eff} - 1 \sim O(1)$. We note that, as the bulk ions are not significantly redistributed when the plasma rotation is subsonic, the qualitative behavior of the transport coefficients is well described by their behavior in the limit $Z_{\rm eff} \to \infty$, that is at very high impurity content, where collisions with impurities dominate and bulk ion self-collisions may be neglected. In particular, the scaling of the coefficients with aspect ratio when $Z_{\rm eff} - 1 \sim O(1)$ is the same as the scaling shown by the coefficients in the limit $Z_{\rm eff} \to \infty$. Hence to continue the analysis of the transport coefficients, we now let $Z_{\rm eff} \to \infty$.

When $A_3 = 0$, $1/L_\perp$ is approximately constant over a flux surface. The expressions for $\bar{\Gamma}_2$ and $\bar{q}_2$ thus reduce to those presented in Ref. 8,

$$\bar{\Gamma}_2 = \frac{p_i I^2}{m_i \hat{\Omega}_i^2} \frac{\langle \tau_{iz}^{-1}\rangle}{L_\perp}\left[\left\langle \frac{n}{b^2} - 1\right\rangle + \frac{\langle b^2/n\rangle - 1}{\langle b^2/n\rangle - f_c}(1 - f_c)\right] \tag{84}$$

and

$$\bar{q}_2 = -\frac{3}{2}T_i\bar{\Gamma}_2 - \frac{p_i I^2 T_i}{m_i \hat{\Omega}_i^2}\langle \tau_{iz}^{-1}\rangle\left\langle \frac{n}{b^2} - f_c\right\rangle A_2. \tag{85}$$

The additional terms that occur for a general $A_3$ are of the same form, but are multiplied by $\langle M_i^2 - (M_z^2/z)\rangle$, so they are smaller by at least a factor $\sim 1/z$.

The neoclassical angular momentum transport coefficients become

$$\bar{l}_{31} = \left\langle \frac{nr^2}{b^2}\right\rangle - f_c\langle nr^2\rangle - \frac{1 - f_c\langle nr^2\rangle}{\langle b^2/n\rangle - f_c}(1 - f_c), \tag{86}$$

$$\bar{l}_{32} = -\frac{3}{2}\bar{l}_{31}, \tag{87}$$

$$\bar{l}_{33}^{(1)} = 2\left\langle M_i^2 - \frac{M_z^2}{z}\right\rangle\left[\left\langle \frac{nr^4}{b^2}\right\rangle - f_c\langle nr^2\rangle^2\right.$$
$$\left. - \frac{(1 - f_c\langle nr^2\rangle)^2}{\langle b^2/n\rangle - f_c}\right], \tag{88}$$

and

$$\bar{l}_{33}^{(2)} = -\frac{5}{2}\frac{R_0^2 B_0^2}{I^2}\left[\frac{15B_0^2}{4}\int_0^{B_{\min}^{-1}}\frac{\langle (nr^2/b)(B_\phi^2 - B_p^2/2/B_0^2)\sqrt{1 - \lambda B}\rangle^2}{\langle n\sqrt{1 - \lambda B}\rangle}\right.$$
$$\left. \times \lambda d\lambda - \left\langle nr^4\left(\frac{B_\phi^2 - B_p^2/2}{B^2}\right)^2\right\rangle\right]. \tag{89}$$

The impurity distribution around a flux surface is expected to have a form such as that given in Eq. (14), which shows that the degree of impurity redistribution scales with $z\varepsilon M_i^2$. We now consider the transport coefficients in the cases

of strong and weak impurity redistributions, restricting to the limit of large aspect ratio. To allow the flux-surface shape to remain arbitrary in the following analysis, we take $a(\theta)$ to be the radial distance from the magnetic axis to a poloidal location on the flux surface, indicated by the angle $\theta$, and define a local inverse aspect ratio $\varepsilon(\theta)$, which is a function of the poloidal location on the flux surface, $\varepsilon(\theta) \propto a(\theta)/R_0 \ll 1$, such that, upon expansion, $r = 1 + \varepsilon(\theta)\cos\theta + O(\varepsilon^2)$ and $b = 1 - \varepsilon(\theta)\cos\theta + O(\varepsilon^2)$. We also define $M_{i0} = M_i(R_0)$. Note that in this limit, the classical transport coefficients are of order $\varepsilon^2$.

### 1. Strong impurity redistribution

When $z\varepsilon M_i^2 \sim O(1)$, the impurities are strongly redistributed, hence $\langle n\cos\theta\rangle \sim O(1)$. The large aspect ratio expansion of the neoclassical angular momentum transport coefficients gives, to leading order in $\sqrt{\varepsilon}$,

$$\bar{l}_{31} = (1 - f_c)\left(1 - \frac{1 - f_c}{\langle 1/n\rangle - f_c}\right), \tag{90}$$

$$\bar{l}_{32} = -\frac{3}{2}\bar{l}_{31}, \tag{91}$$

$$\bar{l}_{33}^{(1)} = 2\left(M_{i0}^2 - \frac{M_{z0}^2}{z}\right)\bar{l}_{31}, \tag{92}$$

and

$$\bar{l}_{33}^{(2)} \sim O(\varepsilon^2). \tag{93}$$

To determine the leading order form of $\bar{l}_{33}^{(2)}$ explicitly, we generalize to $r = 1 + \alpha$ and $b = 1 + \beta$, with $\alpha$ and $\beta \sim O(\varepsilon)$ and free to vary arbitrarily over the flux surface. Thus,

$$\bar{l}_{33}^{(2)} = \frac{2}{5}(\langle n(2\alpha + \beta)^2\rangle - \langle n(2\alpha + \beta)\rangle^2). \tag{94}$$

Therefore, $\bar{l}_{33}^{(2)}$ is zero to first order in $\varepsilon$ and sensitive in second order to only the first-order shape of the flux surfaces. Anticipating a brief discussion of entropy production in Sec. VIII, we note here that the Schwartz inequality shows that $\bar{l}_{33} \geqslant 0$. It may also be used to show that $\langle 1/n\rangle > 1$, as $\langle n\rangle = 1$, so $\bar{l}_{31}$ is positive and therefore the sign of $\bar{l}_{33}^{(1)}$ is determined by the sign of $(M_{i0}^2 - M_{z0}^2/z)$.

The circulating particle fraction is $f_c \sim 1 - O(\sqrt{\varepsilon})$, thus with the classical diffusion coefficient $D_{\rm cl} = \rho_i^2/\tau_{iz}$ and $q$ as the safety factor,

$$L_{31} \sim - L_{32} \sim \frac{q^2 D_{\rm cl}}{\varepsilon^{3/2}}$$

and

$$L_{33} \sim \left(M_i^2 - \frac{M_z^2}{z}\right)\frac{q^2 D_{\rm cl}}{\varepsilon^{3/2}}.$$

The angular momentum flux therefore shows the scaling with aspect ratio charateristic of the banana regime thus it is enhanced by a factor of $\varepsilon^{3/2}$ over previous predictions.[4,9]

The effect of rotation shear, described by the term $A_3$ as a driving force, is increased by $[M_i^2 - (M_z^2/z)]\varepsilon^{-3/2}$ over pre-

vious results, a small factor as $M_i^2 \ll 1$. However, radial pressure ($A_1$) and temperature ($A_2$) gradients become very effective driving forces in the presence of impurities and essentially dominate the transport.

Considering the particle and heat fluxes in this same limit, we find

$$L_{11} \sim -L_{12} \sim \frac{q^2 D_{\mathrm{cl}}}{\varepsilon^{3/2}},$$

$$L_{13} \sim \left(M_i^2 - \frac{M_z^2}{z}\right)\frac{q^2 D_{\mathrm{cl}}}{\varepsilon^{3/2}},$$

$$-L_{21} \sim L_{22} \sim \frac{q^2 D_{\mathrm{cl}}}{\varepsilon^{3/2}},$$

and

$$-L_{23} \sim \left(M_i^2 - \frac{M_z^2}{z}\right)\frac{q^2 D_{\mathrm{cl}}}{\varepsilon^{3/2}}.$$

### 2. Weak impurity redistribution

When $M_i^2$ is strictly of order $1/z$, we expect $z\varepsilon M_i^2 \sim O(\varepsilon)$, so the impurities will be only weakly redistributed. Hence $\langle n \cos \theta\rangle \sim O(\varepsilon)$. Expansion of the coefficients then shows that the scaling of the particle and momentum fluxes is as expected for bulk ions in the Pfirsch-Schlüter regime,

$$L_{11} \sim -L_{12} \sim q^2 D_{\mathrm{cl}},$$

$$L_{13} \sim \left(M_i^2 - \frac{M_z^2}{z}\right)q^2 D_{\mathrm{cl}},$$

$$L_{31} \sim -L_{32} \sim q^2 D_{\mathrm{cl}},$$

$$L_{33} \sim \left(M_i^2 - \frac{M_z^2}{z}\right)q^2 D_{\mathrm{cl}},$$

and only the temperature gradient driven part of the heat flux retains the banana regime scaling, as was found previously when impurity redistribution was neglected,

$$-L_{21} \sim q^2 D_{\mathrm{cl}},$$

$$L_{22} \sim \frac{q^2 D_{\mathrm{cl}}}{\varepsilon^{3/2}},$$

and

$$-L_{23} \sim \left(M_i^2 - \frac{M_z^2}{z}\right)q^2 D_{\mathrm{cl}}.$$

### C. Numerical modeling

Finally in this section we summarize results of numerical calculation of the transport coefficients. The equilibrium flux surfaces of a typical subsonically rotating plasma, in the tight aspect ratio, Mega-Ampère Spherical Tokamak (MAST)[15] were determined from a magnetic reconstruction. The transport coefficients were then evaluated numerically on a flux surface, for a range of assumed toroidal rotation speeds, up to a bulk ion Mach number of 0.5, and impurity contents, as defined by the flux-surface averaged value of $Z_{\mathrm{eff}}$. The distributions of bulk ions, electrons, and impurities around the flux surface were determined to lowest order by solving numerically their coupled, parallel fluid momentum equations, that is equations of the form of Eq. (12). The values of the coefficients at various aspect ratio were determined by evaluating them on different flux surfaces.

The equilibrium was taken from discharge 11 107, 0.19 s into the discharge. The bulk ion density $n_i$ was chosen to be approximately $3 \times 10^{19}$ m$^{-3}$ and $T_i$ was 1 keV, values which are typical for MAST. Fully stripped carbon, $z=6$, was taken to be the single impurity species present in a deuterium plasma, so $m_z = z m_i$. Note that, in this case, $\bar{l}_{13}$, $\bar{l}_{23}$, and $\bar{l}_{33}^{(1)}$ are each zero. For convenience, we define the constant $L_c$ to make $L_{ij}/L_c$ dimensionless,

$$L_{ij} = L_c \left(\frac{I}{1 \text{ T m}}\right)^2 \frac{n_i}{1 \times 10^{19} \text{ m}^{-3}} \frac{\langle n_z\rangle}{1 \times 10^{19} \text{ m}^{-3}}$$

$$\times \left(\frac{T_i}{1 \text{ eV}}\right)^{-1/2} \frac{1}{\langle(B/1 \text{ T})^2\rangle} l_{ij},$$

thus $L_c = (z^2 \ln \Lambda) 2.0 \times 10^{17}$ T$^2$ m s$^{-1}$.

The typical features of the behavior of the neoclassical transport coefficients are demonstrated in Fig. 2(a), which shows $\bar{L}_{31}$ as a function of the bulk ion Mach number $M_{i0} = \langle M_i^2\rangle^{1/2}$ for three values of $\langle Z_{\mathrm{eff}}\rangle$, on a flux surface with an outboard value of the aspect ratio, denoted by $\varepsilon_0 = \varepsilon(\theta=0)$, of 0.32. As $\bar{L}_{31}$ is an off-diagonal term, it is zero in a pure plasma and increases with impurity content. It also increases with Mach number, as the impurity redistribution increases, but the effect is weak for small values of $\varepsilon$, as described earlier in this section.

Figure 2(b) compares the expected levels of particle, heat, and angular momentum transport, characterized by the values of $\bar{L}_{11}$, $\bar{L}_{22}$, $\bar{L}_{31}$, and $\bar{L}_{33}$, respectively, as functions of $M_{i0}$. The impurity content is chosen to give $\langle Z_{\mathrm{eff}}\rangle = 2$, a typical experimental value and $\varepsilon_0 = 0.32$. The dominance of a pressure gradient over rotation shear as a driving force for momentum transport may be seen. The value of $\bar{L}_{33}$ given in Ref. 4 for a pure plasma has previously defined the level of momentum transport expected for all values of $Z_{\mathrm{eff}}$. Here it takes a value around $0.000\,05 L_c$, which barely changes with $M_i$ and cannot be seen on the scale of this graph. Thus we see that the expected level of angular momentum transport is around ten times higher, for $A_1 \sim A_3$, than previously predicted.

In Fig. 2(c) $\bar{L}_{31}\langle B_n^2\rangle/L_c I_n^2$ is shown as a function of $\varepsilon_0$ to demonstrate the scaling of the transport coefficients with aspect ratio at a fixed rotation speed. Here $I_n = (I/1 \text{ T m})$ and $B_n = (B/1 \text{ T})$. A low speed, corresponding to a bulk ion Mach number $M_{i0}$ of 0.2, was chosen. This allows an analytic expression for $\bar{l}_{31}$, depending only on the flux-surface parameters, to be determined, as $n$ may be taken as approximately constant. Using the large aspect ratio expansion discussed at the beginning of this section we find $\bar{l}_{31} \sim 4\varepsilon^2$. This is over-
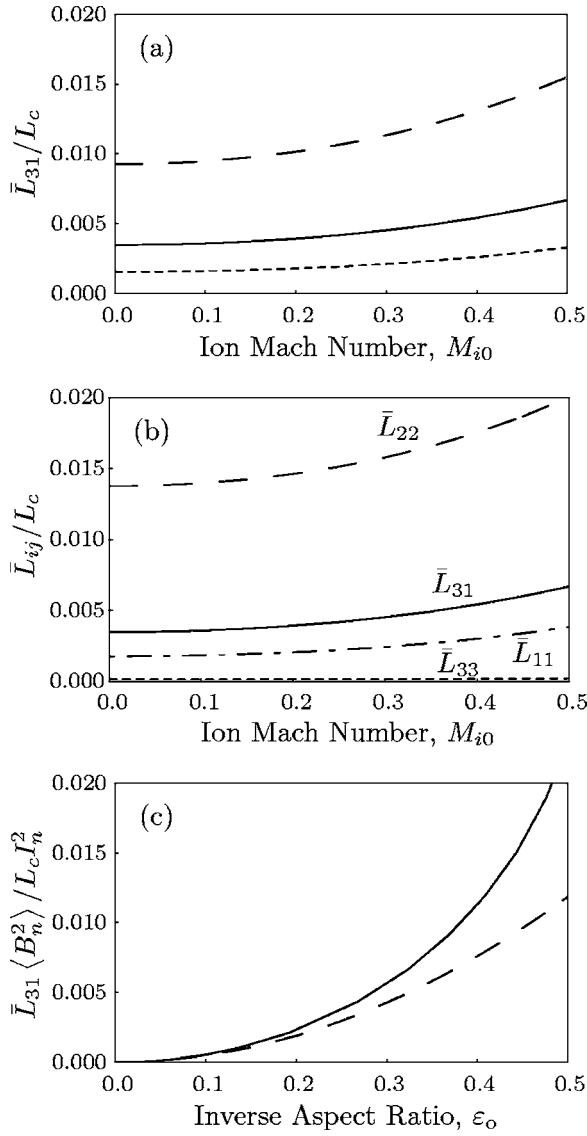
FIG. 2. Summary of results from numerical calculation of the neoclassical transport coefficients. (a) $\bar{L}_{31}$ as a function of the bulk ion Mach number $M_{i0}$ for $\langle Z_{\text{eff}} \rangle = 1.5$ (dotted), $\langle Z_{\text{eff}} \rangle = 2$ (solid), and $\langle Z_{\text{eff}} \rangle = 3$ (dashed) when $\varepsilon_{\text{o}} = 0.32$. (b) Comparison of $\bar{L}_{11}$ (dot-dashed), $\bar{L}_{22}$ (dashed), $\bar{L}_{31}$ (solid), and $\dot{L}_{33}$ (dotted) as functions of $M_{i0}$ when $\langle Z_{\text{eff}} \rangle = 2$ and $\varepsilon_{\text{o}} = 0.32$. (c) $\bar{L}_{31} \langle B_n^2 \rangle / L_c I_n^2$ as a function of inverse aspect ratio (solid) when $M_{i0} = 0.2$, with expected scaling at large aspect ratio overlaid (dashed).
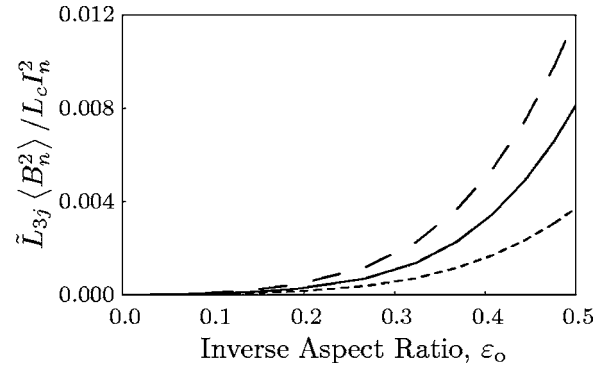


FIG. 3. Classical angular momentum transport coefficients $\tilde{L}_{31} \langle B_n^2 \rangle / L_c I_n^2$ (solid) and $\tilde{L}_{33} \langle B_n^2 \rangle / L_c I_n^2$ (dashed) as a function of inverse aspect ratio when $\langle Z_{\text{eff}} \rangle = 2$ and $M_{i0} = 0.2$. Overlaid is the form of $\tilde{L}_{33} \langle B_n^2 \rangle / L_c I_n^2$ for a pure plasma (dotted).

port by around a factor of 3 by inclusion of impurities. The classical transport remains much smaller than the neoclassical transport.

## VIII. DISCUSSION

Experimentally, the angular momentum transport in regions of neoclassical ion thermal transport has remained anomalous in tokamak plasmas. Motivated by this, we have considered the effect of poloidal redistribution of heavy impurities, due to plasma rotation, on the particle, heat, and angular momentum transport coefficients, in a mixed collisionality plasma characteristic of experiment, that is one consisting of collisionless bulk ions and a highly charged, collisional, impurity species. General forms for the transport coefficients in a subsonically rotating plasma, including the classical contributions, have been derived, which are valid for arbitrary impurity redistribution and flux-surface geometry.

We first note that, in this description, transport is not only driven by radial gradients of the physical observables, bulk ion temperature, and toroidal velocity, but also by the radial gradient of the quantity $N_i$ defined in Eq. (12). This parameter neatly accounts for the radial gradient of the flux-surface averaged bulk ion density $\langle n_i \rangle'$, which one would expect to drive transport, but also the drive produced by the radial dependence of the centrifugal potential, which ions experience whenever the plasma rotates. (The effect of the variation of this potential poloidally due to changes in $R$ has already been taken into account by considering ion redistribution within a flux surface.) Ions may reduce their potential energy, and so evolve towards thermodynamic equilibrium, by moving radially in this centrifugal potential, on the transport time scale. Hence, in the formulation presented, there can still be transport in a plasma in which the usual driving forces, $\langle n_i \rangle'$, $T_i'$, and $\omega'$, are zero if the plasma rotates. To make this idea more explicit, it is useful to consider a homogeneous, nonrotating plasma, in which case the above gradients are zero. If the plasma is then spun up as a rigid body, $T_i'$ and $\omega'$ remain zero, whilst $\langle n_i \rangle'$ can evolve away from zero if there is transport, but it initially provides no driving force. The rotation generates a radially dependent centrifugal force.

laid as a dashed line on the graph and the two curves can be seen to agree well up to a value of $\varepsilon_{\text{o}}$ around 0.3.

Finally, Fig. 3 indicates the expected level of classical transport for comparison. As can be seen from Eqs. (42)–(44), the levels of classical particle, heat, and angular momentum transport are similar. Shown in the figure are $\tilde{L}_{31} \langle B_n^2 \rangle / L_c I_n^2$ and $\tilde{L}_{33} \langle B_n^2 \rangle / L_c I_n^2$ as functions of inverse aspect ratio for $\langle Z_{\text{eff}} \rangle = 2$ and $M_{i0} = 0.2$. Note that they are of similar magnitude in an impure plasma and no driving force is dominating the transport. There is an enhancement by around a factor of 2 when moving from conventional to tight aspect ratio. Overlaid is the form of $\tilde{L}_{33} \langle B_n^2 \rangle / L_c I_n^2$ for a pure plasma (where $\tilde{L}_{31}$ is zero), indicating an enhancement of the trans-

This causes ion redistribution within a flux surface, thus typically creating a local driving force $n_i'$ which is encapsulated in the transport coefficients. It also creates a radial potential between flux surfaces, further driving radial ion motion. An efficient description of the latter effect, along with any drive from $\langle n_i \rangle'$, is achieved by using the parameter $N_i'$.

Before summarizing the properties of the transport coefficients, a point concerning entropy production will be noted. Restrictions on the sign of the diagonal elements of the transport matrix arise in order to ensure that the total surface-averaged neoclassical entropy production is positive. In terms of conjugate fluxes and forces, we require[16]

$$\sum_a \langle \bar{\sigma}_a \rangle = - \sum_a \left( \bar{\Gamma}_a A_{1,a} + \frac{\bar{q}_a}{T_a} A_{2,a} + \frac{\bar{\Pi}_a}{T_a} A_{3,a} \right) \geqslant 0,$$

where $\bar{\sigma}_a$ is the neoclassical entropy production for species $a$, and the driving terms $A_i$ now have an additional subscript as they refer to the parameters of a particular species, for example, $A_{2,a} = T_a'/T_a$. Thus, $\bar{L}_{11}$ and $\bar{L}_{22}$ must be positive. The driving force $A_{3,a}$, conjugate to the angular momentum flux, is the same for both the bulk ions and the impurities to leading order, so it is only necessary for the sum $\sum_a (\bar{L}_{33,a}^{(1)} + \bar{L}_{33,a}^{(2)})/T_a$ to be positive, remembering the separation of $\bar{\Pi}$ into two parts which was introduced in Sec. VI. The electron angular momentum flux may be consistently neglected due to the small electron mass, so the sum here runs over the bulk ions and impurities. Hence, from Eq. (70), it may be seen that

$$\sum_a \bar{\Pi}_a^{(1)} = - \left( m_i - \frac{m_z}{z} \right) \left\langle \frac{I}{eB} \omega R^2 R_{i\parallel} \right\rangle,$$

and therefore

$$\sum_a \frac{\bar{L}_{33,a}^{(1)}}{T_a} = \left( m_i - \frac{m_z}{z} \right) \frac{\bar{L}_{33}^{(1)}}{m_i T_i},$$

where $\bar{L}_{33}^{(1)}$ is given in Sec. VII and we have again taken $T_i = T_z$. Thus, in the limit of strong impurity redistribution, it may be seen from Sec. VII B that the sums $\sum_a \bar{L}_{33,a}^{(1)}$ and $\sum_a \bar{L}_{33,a}^{(2)}$ are individually positive, whilst furthermore each of the terms in the latter sum are positive.

The forms of the classical contributions to the transport coefficients remain valid for arbitrary rotation velocities. No single driving force dominates the classical transport (the on- and off-diagonal components of the transport matrix are comparable) and it shows an enhancement with increasing impurity redistribution over previous expectations, which will be most significant in spherical tokamaks. The mechanism of this enhancement may be understood as being due to the localization of collisions at the outboard side, where the step size for classical transport, as a result of the low magnetic-field strength, and the angular momentum carried per particle are greatest.

In a pure plasma, and in the case of weak impurity redistribution, defined by $z\varepsilon M_i^2 \sim O(\varepsilon)$, the scaling of the heat flux with aspect ratio is characteristic of bulk ions in the banana regime, but both the particle and angular momentum fluxes scale in the manner expected for bulk ions in the collisional, Pfirsch-Schlüter regime. Such scaling of the angular momentum transport may be understood in the following way in a pure plasma, where it is driven purely by toroidal rotation shear. Trapped particles have a net toroidal motion by virtue of the $\mathbf{E} \times \mathbf{B}$ drift they experience, which causes their bounce points to precess at the local rotation frequency. When a trapped particle suffers a collision and moves onto a new trapped orbit, its toroidal rotation frequency is immediately determined by the local $\mathbf{E} \times \mathbf{B}$ drift, so there is no net transfer of angular momentum. The effect of the $\mathbf{E} \times \mathbf{B}$ drift on passing particles is negligible during an orbit, but they are forced to rotate toroidally with the same frequency due to the friction between the passing and trapped particles. Therefore, when a passing particle suffers a collision and moves onto a new passing orbit, the memory of its previous rotation velocity must be removed by the friction between this and local particles. As the typical excursion of a passing particle from a flux surface is $q\rho_i$, the momentum diffusivity would be expected to be of the order of $\nu_{ii} q^2 \rho_i^2$, as was found above.

At large aspect ratio, when the impurities are strongly redistributed, $z\varepsilon M_i^2 \sim O(1)$, all three radial fluxes are found to show the scaling with aspect ratio expected for collisionless bulk ions. The off-diagonal terms describing angular momentum transport are enhanced by a factor of $\varepsilon^{-3/2}$, causing the angular momentum flux to be of the order of the ion heat transport, as is often observed experimentally. Equations (65) and (70) show that the enhanced angular momentum transport is due to the enhancement of the particle flux and the associated loss of the angular momentum carried by an individual particle from a flux surface. This effect may be understood as follows. The radial particle flux is driven by the friction between the ions and impurities. Normally, when the plasma does not rotate toroidally, this friction is relatively small, as the impurity ions rotate poloidally in such as a way as to minimize it. Specifically, Eq. (23) reduces to $\langle R_{z\parallel} \rangle = 0$ in the limit of large aspect ratio and small toroidal rotation speed. However, when the toroidal rotation is taken to be so large that the impurities are localized towards the outboard side of each flux surface, their poloidal flow velocity is decreased, see Eq. (64), so they are unable to follow the ions poloidally. Thus the friction between the two species, and hence the particle flux, is increased.

Radial pressure and temperature gradients are the primary driving forces of the fluxes in this limit of strong redistribution ($(L_{31} \sim L_{32} \gg L_{33})$). The pressure and temperature gradients formed in the region of an ITB can thus drive a momentum flux, which may be able to maintain the electric-field shear creating the barrier and helping to make the transport barrier self-sustaining. Furthermore, the large values of $L_{31}$ and $L_{32}$ could allow spontaneous toroidal rotation to arise in a plasma, as is frequently observed in experiments,[2] since there is no external source to balance $\Pi$,

$$\frac{\omega'}{\omega} = - \frac{1}{L_{33}} \left( L_{31} \frac{p_i'}{p_i} + L_{32} \frac{T_i'}{T_i} \right). \tag{95}$$

The magnitude and direction of the rotation will depend on the edge boundary condition.

Finally, we note that $\bar{L}_{21}$ and $\bar{L}_{23}$ describe heat pinches, driven by the pressure gradient and rotation shear, respectively, which may help to account for observed subneoclassical levels of heat transport.[17]

## ACKNOWLEDGMENTS

[1] C. M. Greenfield, C. L. Rettig, G. M. Staebler *et al.*, Nucl. Fusion **39**, 1723 (1999).

[2] J. E. Rice, W. D. Lee, E. S. Marmar *et al.*, Nucl. Fusion **44**, 379 (2004).

[3] M. N. Rosenbluth, P. H. Rutherford, J. B. Taylor, E. A. Frieman and L. M. Kovrizhnykh, *Plasma Physics and Controlled Nuclear Fusion Research* (International Atomic Energy Agency, Vienna, 1971), Vol. 1, p. 495.

[4] F. L. Hinton and S. K. Wong, Phys. Fluids **28**, 3082 (1985).

[5] P. J. Catto, I. B. Bernstein, and M. Tessarotto, Phys. Fluids **30**, 2784 (1987).

[6] S. P. Hirshman, Phys. Fluids **19**, 155 (1976).

[7] J. A. Wesson, Nucl. Fusion **37**, 577 (1997).

[8] T. Fülöp and P. Helander, Phys. Plasmas **6**, 3066 (1999).

[9] S. K. Wong, Phys. Fluids **30**, 818 (1987).

[10] P. Helander and D. J. Sigmar, *Collisional Transport in Magnetized Plasmas* (Cambridge University Press, Cambridge, 2002), p. 55.

[11] S. I. Braginksii, Sov. Phys. JETP **6**, 358 (1958).

[12] P. Helander, Phys. Plasmas **5**, 3999 (1998).

[13] S. P. Hirshman and D. J. Sigmar, Nucl. Fusion **21**, 1079 (1981).

[14] P. Helander, Phys. Plasmas **5**, 1209 (1998).

[15] R. J. Akers, J. W. Ahn, G. Y. Antar *et al.*, Plasma Phys. Controlled Fusion **45**, A175 (2003).

[16] H. Sugama and W. Horton, Phys. Plasmas **4**, 2215 (1997).

[17] F. M. Levinton, M. C. Zarnstorff, S. H. Batha *et al.*, Phys. Rev. Lett. **75**, 4417 (1995).